Solid State Science and Technology, Vol. 17, No 1 (2009) 229-236
ISSN 0128-7389

GRAIN – MATRIX MOSAIC CONTRIBUTION TO ac LOSSES IN Ni – DOPED BSCCO CYLINDERS

M.I. Adam, S.A. Halim, M.A.M. Faisal, H. Baqiah and M. Kamarulzaman

Superconductor and Thin film Laboratory, Department of Physics, Faculty of Science, 43400 UPM, Serdang, Selangor, D E. MALAYSIA

ABSTRACT

The measurements of ac susceptibility $\chi = \chi' + i\chi''$ is performed to determine the characteristics of intergranular components in sintered $Bi_{1.6}Pb_{0.4}Sr_2(Ca_{1-x}Ni_x)_2Cu_3O_\delta$, (x = 0.0 – 0.05) polycrystalline cylinders prepared by the conventional route. Theoretical values of χ''_{max} for idealized cylinder were calculated in the range $0 \le k \le 1$, correspondence of the Bean and the simplified Kim critical state models. Magnetization curve for various stages in the specimens is hence approximated. It is found that Ni content in BSCCO system changes the effective volume fraction of the grains, field dependence of the intergranular critical current density, transition temperature, and the intergranular pinning property.

INTRODUCTION

The intrinsic property of superconducting grains is a twin component to the grains' coupling property in textured high-T_c ceramics. However, each of the twin property has its independent signature in the overall response of the constituent material to electromagnetic application. The coupling property normally responds weakly to superconductivity and the applied magnetic field penetrates easily through it compared to the grain property. Constitution of high-T_c ceramics is made of a collection of tiny, randomly oriented anisotropic grains connected by a system of matrix. The grains in the ceramics are characterized by comparatively high values of critical current density and critical field H_{c1}. The system of intergranular links, (matrix) shows considerably lower values of these parameters. The dissipation phenomenon in these materials is thus governed by the microstructure developed during preparation process. Therefore, detailed investigations of magnetization and ac magnetic susceptibility in superconductors prepared by either form of single crystal, thin films or polycrystalline are important for understanding superconductivity as well as for practical applications.
The area enclosed by hysteresis loop <M>, the spatial average of magnetization, versus H_{ac} , the external applied magnetic field is a measure of dissipated energy per cycle of H_{ac} and the ac susceptibility is intimately tied to the ac losses. High-T_c superconductors exhibit various loss mechanisms [1-4] such as eddy-current losses, flux- flow losses, bulk-pinning hysteretic losses, surface pinning hysteretic losses and flux-line cutting losses.

On the other hand, low field ac susceptibility measurements are very important for the

Corresponding Author: mdries@hotmail.com

Solid State Science and Technology, Vol. 17, No 1 (2009) 229-236
ISSN 0128-7389

characterization of high-T_c superconductors [5-8]. The sharp decrease in the real part $\chi'(T)$ below the critical temperature T_c is a manifestation of diamagnetic shielding and the peak in the imaginary part $\chi''(T)$ is representing the ac losses. The shapes of ac loss peaks $\chi''(T)$ are strongly influenced by the thermal treatments and fabrication process, the class and morphology of the samples, the measuring conditions and grain matrix mosaic in granular superconductors. Due to the technological importance of ac losses, it is of interest to study this subject in doped BSCCO superconductors. In this article, we report on the effects of Ni doping contribution to the grain – matrix mosaic losses in $Bi_{1.6}Pb_{0.4}Sr_2(Ca_{1-x}Ni_x)_2Cu_3O_{ä}$ ceramics.

EXPERIMENTAL PROCEDURE

Samples with nominal composition $Bi_{1.6}Pb_{0.4}Sr_2(Ca_{1-x}Ni_x)_2Cu_3O_{\delta}$, were prepared by the conventional route where x = 0.0 - 0.05. Stoichiometric amounts of Bi_2O_3, PbO, $SrCO_3$, $CaCO_3$, CuO and nickel oxide of purity up to 99.9% were used as starting materials. Required quantities of the materials were weighed using digital balance of 10^{-4} mg accuracy. The weighed powders were mixed up and ball-milled in alcohol medium for 24 hours. The mixture was dried out in an oven at 120 $^{\circ}$C for 6 hours and ground. The mixture was first calcined at 800 $^{\circ}$C for 20 hours. Calcination steps were extended at 820 and 840 $^{\circ}$C for 10 and 5 hours with intermediate grinding, respectively. The resulting powder was ground and pulverised using a standard sieve of 25µ. A mass of 1.2 g from the homogeneous powder was pressed into disc-shaped pellet and sintered in air at 855 $^{\circ}$C for 150 hours. Further annealing step was done at 830 $^{\circ}$C for 30 hours and then the pellet samples were cooled in air environment with a rate of 2°C/min to the ambient temperature.

The ac susceptibility of the cylinders was measured with a commercial Lake Shore susceptometer model 7000. The dimensions (2a×2b×c) of the cylinders for ac susceptibility measurements do not change with the sample and are nearly identical to $1.80\times2.15\times12.35 mm^3$. The cylinder was mounted such that its length was along the direction of the magnetic field. The temperature variation was enhanced using a closed cycle helium cryostat equipped with a temperature controller. The signal due to the in-phase and out-of-phase magnetization was taken simultaneously.

RESULTS AND DISCUSSION

Figure 1 shows the ac loss peaks measured at H_{ac}= 400 A/m (rms) and f=125 Hz for the cylinders A (x =0.0), B (x =0.01), C (x =0.02), D (x =0.03), E (x =0.04), F (x =0.05). Note that Ni doping to BSCCO system plays an important role on the grain- matrix mosaic. The height of both intragranular and intergranular peaks, peak temperatures and the patterns of ac loss peaks vary with Ni content. There are two contributions to the experimental ac susceptibility data. The principle of separation of these contributions from grains and coupling matrix is described elsewhere [9].

Corresponding Author: mdries@hotmail.com

Solid State Science and Technology, Vol. 17, No 1 (2009) 229-236
ISSN 0128-7389

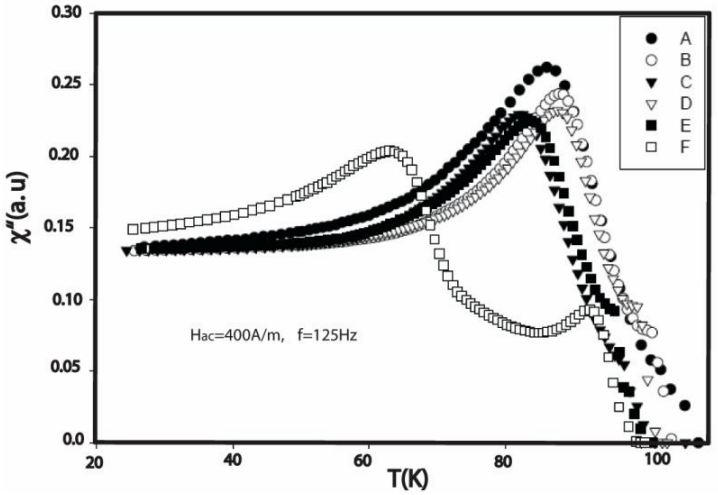

Figure 1: Measured susceptibility $\chi''(\mathrm{T})$ for the cylinders shown in the legend.

The experimental matrix susceptibility χ'_m and χ''_m were extracted from the measured susceptibility employing the following equations [11]:

$$\chi'' = (1 - f_g)\chi''_m \qquad (1)$$

$$\chi' = -f_g + (1 - f_g)\chi'_m \qquad (2)$$

The matrix susceptibility is determined from Eqns. (1) and (2) using the value of *fg* for each cylinder. The volume fraction of the grains *fg* is estimated from Figure 2 which shows the $\chi'(\chi'')$ data for all cylinders measured at H_{ac}= 400 A/m (rms) and f=125 Hz. The extrapolated onset in $\chi'(\chi'')$ graph roughly indicates the values of *fg* for each cylinder [8]. Hence, we used the *fg* values determined by the above procedure for the calculation of the matrix susceptibility listed in Table 1.

Table 1: Superconducting parameters of $Bi_{1.6}Pb_{0.4}Sr_2(Ca_{1-x}Ni_x)_2Cu_3O_{ä}$ cylinders.

PARAMETER	**CYLINDER**					
	A	**B**	**C**	**D**	**E**	**F**
χ''_{max}	0.262	0.244	0.229	0.232	0.225	0.204
$\chi'(T_P)$	- 0.549	-0.642	-0.662	-0.667	-0.662	-0.683
f_g	0.28	0.38	0.31	0.40	0.35	0.42
$\chi''_{m,max}$	0.366	0.393	0.332	0.386	0.346	0.354
k	0.80	0.98	0.60	0.92	0.70	0.40
T_c	108.5	105.3	102.0	103.0	101.0	99.0

Like most bulk high – T_c superconductors, the cylinders we treat here are fabricated by sintering compressed powders of chosen composition. These materials are not only polycrystalline but exhibit granular behaviour. In these materials, individual grains can carry large depinning critical current densities, j_{cg}.The lossless current carrying capacity of the bulk specimens, hence the resultant critical conduction current density, j_{cm} in this work, is considerably smaller than j_{cg} measured for individual grains. j_{cm} is the

Corresponding Author: mdries@hotmail.com

intergrain critical current density .The critical state ideas can be applied separately to the individual grains to estimate the intragranular critical current density [10]. In order to pursue these concepts quantitatively however, several approximations and simplifications were introduced. This work only focuses on the intergranular pinning properties.

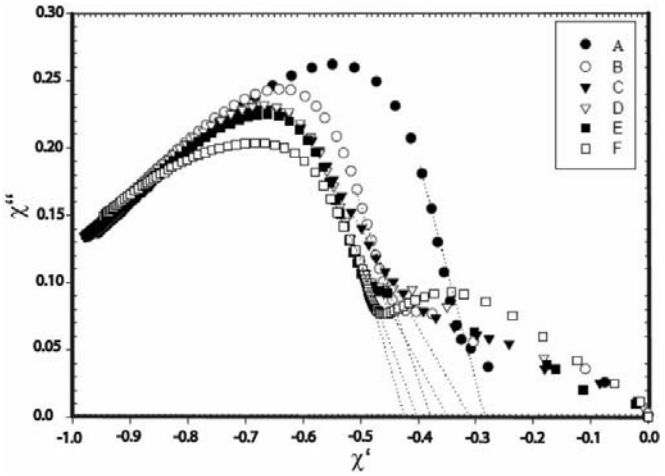

Figure 2: The $\chi'(\chi'')$ plot at H_{ac} = 400A/m. Extrapolated dots roughly indicate the values of f_g.

Figure 3 displays the extracted matrix susceptibility vs temperature at H_{ac}=400 A/m and f=125 Hz for all cylinders. Note that we removed the data corresponding to intragranular contribution. For the samples of cylinder shape, according to the Bean model [11] the theoretical value of χ''_{max} is equal to 0.212 and the corresponding value of χ' is -0.333. The extracted values of maximum of the matrix susceptibility for all cylinders differ from the theoretical values for the Bean-cylinder case (see Table I).

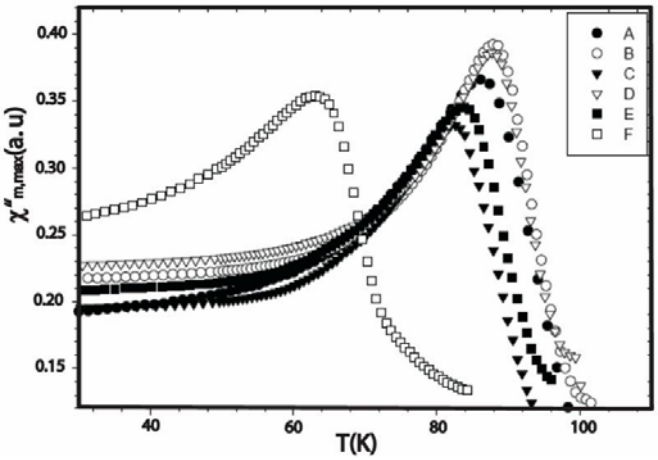

Figure 3: Extracted matrix susceptibly vs temperature at H_{ac} = 400A/m for all cylinders

Hence, we calculated the theoretical value of χ''_{max} for idealized cylinder geometry employing the power law model for $0 \leq k \leq 1$. The range of the inequality corresponds

Corresponding Author: mdries@hotmail.com

Solid State Science and Technology, Vol. 17, No 1 (2009) 229-236
ISSN 0128-7389

to the Bean model and the simple Kim model, where

$$j_c = \frac{j_{c0}}{\left(\mathrm{H}/\mathrm{H}_{ref}\right)^k} \qquad (3)$$

is introduced in (<M> -H) loop calculations. Here the parameter H_{ref} is introduced so that the important quantity j_{co} has the units of current density. We then calculated the magnetization curves of the cylinders for various stages [12]. For a cylinder of radius R with its axis parallel to an applied field Ha, within the critical state model and Maxwell 's equation $\nabla \times H = j_c$, the magnetization <M> is given by

$$<\mathrm{M}> = \frac{2}{R^2}\int_0^R \mathrm{H}(r)\ r dr - \mathrm{H}_a \qquad (4)$$

Corresponding description for a complete loop uses the flux density profile $\mathrm{H}^{\pm}(r)$, respectively:

$$\mathrm{H}^{+}(r) = \left[\left(\mathrm{H}_a^{k+1} - \mathrm{H}_*(1 - r/R)\right]^{\frac{1}{k+1}} \qquad (5)$$

$$\mathrm{H}^{-}(r) = \left[\left(\mathrm{H}_a^{k+1} + \mathrm{H}_*(1 - r/R)\right]^{\frac{1}{k+1}} \qquad (6)$$

Note that Eqns. (5) and (6) are the manifestation of the induced critical current during upswing or downswing of the magnetic field, which flows through the cylinder in clockwise and counterclockwise direction. We have calculated the magnetization <M> as a function of applied field H_a in the small increment of ΔH_a. Thus the locus of complete hysteresis loop is mapped out in the (<M> - $H_{a)}$ plane for a specific choice of k. The area enclosed by each hysteresis cycle A_H is computed by summing up the differences between corresponding pairs of <M> values shown in Fig. 4. The imaginary part of the fundamental ac susceptibility is a direct measure of the ac hysteresis losses,

$$\chi'' = \frac{\mathrm{A}_{\mathrm{H}}}{\pi \mathrm{H}_{ac}^2} \qquad (7)$$

Therefore, we calculated and plotted $\chi''_{\max}$ values as a function of k in Fig. 5. To estimate the field dependence of the intergranular critical current density, we used the $\chi''_{m,\max}$ values as criteria. The determined k values are listed in Table 1 for each cylinder. Note that $\chi''_{m,\max}$ corresponds to f=125 Hz and although there could be frequency dependence in a small extent, we ignored the frequency dependence of $\chi''_{m,\max}$ for simple comparison.

Corresponding Author: mdries@hotmail.com

Solid State Science and Technology, Vol. 17, No 1 (2009) 229-236
ISSN 0128-7389

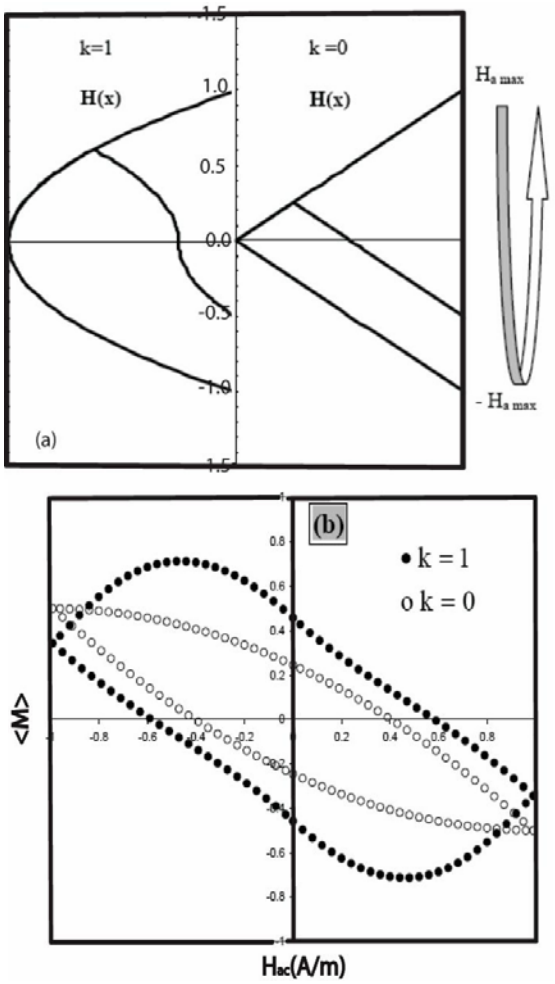

Figure 4: (a) Schematic of the evolution of the magnetic field profile in an ideal cylinder of radius R. (b) calculated (<M> - H_a) hysteresis loop for K= 0 and 1 are correspondence of the Bean' and the simplified Kim models.

Corresponding Author: mdries@hotmail.com

Solid State Science and Technology, Vol. 17, No 1 (2009) 229-236
ISSN 0128-7389

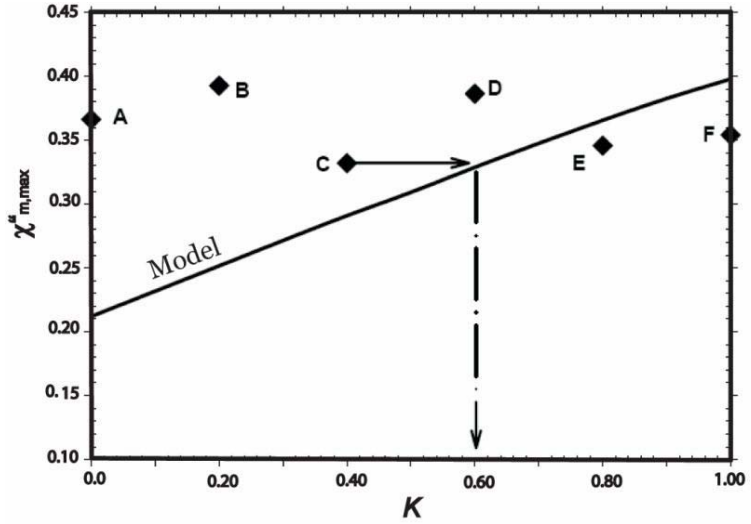

Figure 5: Calculated values of $\chi''_{m,\max}$ vs. k for field dependence on the models' line.

CONCLUSION

We have investigated the effect of Ni-doping on the intergranular flux pinning properties of Bi(Pb)-Sr-Ca-Cu-O ceramic superconductors. From the comparative analysis and determination of some parameters, the following conclusions can be drawn. After estimation of the volume fraction of the grains from ac susceptibility data, we calculated the temperature dependent ac matrix susceptibility for all cylinders. It is found that Ni content in the BSCCO system changes both the effective volume fraction of the grains and the field dependence of the intergranular critical current density as well as the transition temperature and intergranular pinning properties

ACKNOWLEDGEMENT

This work is supported by the Research University Grant Scheme (RUGS/ Vote. 90010) of the Research Management Centre, RMC at UPM.

REFERENCES

[1]. J. R Clem, (1992). in *Magnetic Susceptibility of Superconductors and Other Spin Systems* edited by R. A. Hein,T.L. Francavilla, D. H. Liebenberg, , New York, Plenim.
[2]. J. R Clem, (1982). Phys. Rev. B, **26**, 2463.
[3]. J. R Clem. and A P.Gonzalez., (1984). *Phys. Rev. B,* **30**, 5041.
[4]. S. Celebi, A. I. Malik, F. Inanir, and S. A. Halim, (2004) *J. Alloys and Compounds*, **370**, 69.
[5]. D. X. Chen, J. Nogues, and K. V. Rao, (1989). *Cryogenics*, **29**, 800
[6]. K. H Muller, (1989). Physica C,**159**, 717.

Corresponding Author: mdries@hotmail.com

[7]. T. Ishida and R. B. Goldfarb, (1990). *Phys. Rev. B*, **41**, 8937.
[8]. S. Celebi, (1999). *Physica C* **316**, 251.
[9]. J. R.Clem, (1988). *Physica C* **153**, 50.
[10]. D-X. Chen and A. Sanchez, (1992). *Phy. Rev. B*, **45**, 10793.
[11]. C. P. Bean, (1964). *Rev. Mod. Phys*. **36** 31.
[12]. M.A.R.LeBlanc, G. Fillion, and J. P. Lorrain, (1986). *J. Appl. Phys*. **59**, 3208.

Corresponding Author: mdries@hotmail.com